

# Effects of correlation between merging steps on the global halo formation

Jun Pan<sup>1\*</sup>, Yougang Wang<sup>2</sup>, Xuelei Chen<sup>2</sup>, and Luís Teodoro<sup>3</sup>

<sup>1</sup> *The Purple Mountain Observatory, 2 West Beijing Road, Nanjing 210008, China*

<sup>2</sup> *National Astronomical Observatories, Chinese Academy of Sciences, Beijing 100012, China*

<sup>3</sup> *Department of Physics and Astronomy, University of Glasgow, Glasgow G12 8QQ, UK*

6 November 2018

## ABSTRACT

The excursion set theory of halo formation is modified by adopting the fractional Brownian motion, to account for possible correlation between merging steps. We worked out analytically the conditional mass function, halo merging rate and formation time distribution in the spherical collapse model. We also developed an approximation for the ellipsoidal collapse model and applied it to the calculation of the conditional mass function and the halo formation time distribution. For models in which the steps are positively correlated, the halo merger rate is enhanced when the accreted mass is less than  $\sim 25M^*$ , while for the negatively correlated case this rate is reduced. Compared with the standard model in which the steps are uncorrelated, the models with positively correlated steps produce more aged population in small mass halos and more younger population in large mass halos, while for the models with negatively correlated steps the opposite is true. An examination of simulation results shows that a weakly positive correlation between successive merging steps appears to fit best. We have also found a systematic effect in the measured mass function due to the finite volume of simulations. In future work, this will be included in the halo model to accurately predict the three point correlation function estimated from simulations.

**Key words:** cosmology: theory – large scale structure of the Universe – galaxies : halos – methods : analytical

## 1 INTRODUCTION

The excursion set theory provides a simple and intuitive model for cosmic structure formation. In this theory, as one varies the smoothing scale  $R$ , the linear density fluctuation  $\delta_R$  obtained with smoothing window  $W(R)$  forms a one dimensional random walk. It is deemed that the non-linear halo formation and evolution history can be treated with the corresponding excursion set theory: a halo is formed when a pre-set barrier  $\delta_c(z)$  is exceeded by a trajectory of the random walk.

It is convenient to take the variance of the random density field  $S(R) = \sigma^2(R)$  as the pseudo-time variable. Properties of the random walk rely on the window function used and the nature of the primordial fluctuation. For Gaussian fluctuations and using the sharp k-space filter, the random walk produced by smoothing is a normal Brownian motion (hereafter NBM), i.e. there is no correlation between steps. The density of trajectories  $Q(S, \delta)$  passing through  $(S, \delta)$

then satisfies a diffusion equation

$$\frac{\partial Q}{\partial S} = \frac{1}{2} \frac{\partial^2 Q}{\partial \delta^2} \quad (1)$$

From  $Q(S, \delta)$  one could derive the halo mass function and merger rates, etc. (Bond et al. 1991; Lacey & Cole 1993).

However, although the N-body simulation results generally agree with the predictions of the excursion set theory, there are significant deviations in the details. The discrepancy is particularly severe in the description of small mass halos. This discrepancy can be partly overcome by replacing the spherical collapse model with ellipsoidal collapse model, i.e. by introducing a moving barrier instead of a fixed barrier imposed on the random walk (e.g. Sheth & Tormen 2002). This practical approach provides a reasonably good fitting formula for halo mass function (Warren et al. 2006), but its prediction on the formation time distribution of low- and intermediate-mass halo remains unsatisfactory (Giocoli et al. 2007). One suspects that if correlations between steps of the random walk is introduced, the excursion set theory might be improved. Indeed, if the smoothing window function is not a sharp k-space filter but

\* jpan@pmo.ac.cn

a Gaussian filter or a real space tophat filter, the excursion steps would be correlated.

In a previous work by the leading author, the fractional Brownian motion (FBM), the simplest random walk with steps correlated in long range, was introduced to generalize the excursion set theory. The correlation between steps of the random walk was shown to be capable of modifying the final halo mass function in a non-trivial way (Pan 2007). The model presented there was incomplete though, as the solution for ellipsoidal collapses and the treatment of halo merging history were not discussed. These are the topics of the present report.

This paper is organized as follows. In section 2 we fit the FBM into the excursion set theory to account for the possible correlated halo formation process. Then in section 3 the diffusion equation of FBM is solved in the spherical collapse model, and we calculate the conditional mass function, halo merger rate and the halo formation time distribution with the modified theory. Treatment to the ellipsoidal collapse is given in section 4, together with a comparison between theoretical predictions and measurements with simulations. The final section contains our conclusions and discussion. We adopt the flat  $\Lambda$ CDM model with the following set of cosmological parameter values:  $\Omega_m = 0.3$ ,  $\Omega_\Lambda = 0.7$ ,  $h = 0.7$  and  $\sigma_8 = 0.9$ .

## 2 MODELING CORRELATED MERGING STEPS

### 2.1 The diffusion equation

To work out the halo conditional mass function, the central element is the diffusion equation which governs the behavior of the random walk. Such diffusion equation in turn depends on the understanding of the random walk with which the physical problem is concerned with. The conditional mass function is in fact a two-barriers crossing problem of a random walk, which means the key object we shall check is the scaling relation between  $\delta(S_1) - \delta(S_0)$  and  $S_1 - S_0$ .

The FBM is a random process  $X(t)$  on some probability space such that:

- (i)  $X(t)$  is continuous and  $X(0) \equiv 0$ ;
- (ii) for any  $t \geq 0$  and  $\tau > 0$ , the increment  $X(t+\tau) - X(t)$  follows a normal distribution with mean zero and variance  $\tau^{2\alpha}$ , so that

$$P(X(t+\tau) - X(t) \leq x) = \frac{\tau^{-\alpha}}{\sqrt{2\pi}} \int_{-\infty}^x e^{-u^2/2\tau^{2\alpha}} du. \quad (2)$$

The parameter  $\alpha$  is the Hurst exponent, if  $\alpha = 1/2$ , it is reduced to the normal Brownian motion (c.f. Feder 1988). It is also easy to see that the following is satisfied by the FBM:

$$\begin{aligned} \langle [X(t+\tau) - X(t)]^2 \rangle &= \tau^{2\alpha} \\ \langle X(t) [X(t+\tau) - X(t)] \rangle &= \frac{(t+\tau)^{2\alpha} - t^{2\alpha} - \tau^{2\alpha}}{2}, \end{aligned} \quad (3)$$

With this definition of FBM, the trajectory density  $Q_\alpha(X, t)$  at time  $t$  in interval  $(X, X+dX)$  follows the diffusion equation (c.f. Lutz 2001),

$$\frac{\partial Q_\alpha}{\partial t} = D \frac{\partial^2 Q_\alpha}{\partial X^2}, \quad D = \frac{1}{2} \frac{d}{dt} \langle X(t)^2 \rangle = \alpha t^{2\alpha-1}. \quad (4)$$

Why invoke FBM? The trajectory of  $\delta(S)$  is characterized by properties of the increments  $\delta(S_1) - \delta(S_0)$  between any pairs of  $(S_0, S_1 > S_0)$ . If the smoothing window function corresponding to halo definition is not a sharp k-space filter but e.g. a Gaussian or top-hat, it is easy to check that  $\langle [\delta(S_1) - \delta(S_0)]^2 \rangle$  is not  $S_1 - S_0$  but proportional to  $(S_1 - S_0)^\alpha$  with a constant  $\alpha$  in broad scale range. The scaling relation is the flagging attribute of the FBM<sup>1</sup>, so it is reasonable to install the FBM into the excursion set theory as the simplest approach to analytically inspect halo models constructed with random walks with correlated steps.

On the other hand, we know in practice that the boundary, and subsequently the mass of a halo identified in a simulation is rather arbitrary, e.g. the mass picked up is often defined by a halo's virial radius while the mass outside is simply not counted. The  $S$  from the virial mass  $M$  is very likely not the real place where the particular random walk corresponding to the halo hit the barrier. In fact Cuesta et al. (2007) argued that if one replaces the virial mass with the static mass, the mass function agrees with the Press-Schechter formula remarkably well, rather than the Sheth-Tormen one, and the ratio of the virial mass to the static mass depends on redshift and halo mass.

While the true scale can be smaller or larger than the  $S$  inferred from  $R(M)$ , one can always parametrize the true scale with  $S(R)$  so that  $\langle \delta^2 \rangle = S^{2\alpha}$ . Taking the approximation that  $\alpha$  is a constant not too far away from  $1/2$ , we can comfortably assume the applicability of the FBM.

For an FBM with  $\langle \delta^2 \rangle = S^{2\alpha}$ , by Eq. (3), the variance of the increments at two points  $(S_0, S_1 > S_0 > 0)$  satisfies

$$\begin{aligned} \langle [\delta(S_1) - \delta(S_0)]^2 \rangle &= (S_1 - S_0)^{2\alpha}, \\ &\text{with } \alpha \in (0, 1), \quad S_1 > S_0 > 0, \end{aligned} \quad (5)$$

so that a new trajectory is formed by  $\tilde{\delta}(\Delta S) = \delta(S_1) - \delta(S_0)$  along  $\Delta S = S_1 - S_0$ , given any source point  $(S_0, \omega_0 = \delta_0(S_0))$ . Apparently the new random walk also complies with the definition of FBM, its diffusion equation being

$$\frac{\partial Q_\alpha}{\partial \Delta S} = \mathcal{D}_{\Delta S} \frac{\partial^2 Q_\alpha}{\partial \tilde{\delta}^2}, \quad \mathcal{D}_{\Delta S} = \frac{1}{2} \frac{d \langle \tilde{\delta}^2 \rangle}{d \Delta S} = \alpha \Delta S^{2\alpha-1}. \quad (6)$$

It is this diffusion equation that ought to be solved to figure out the conditional mass function, which can be further transformed to the familiar diffusion equation of normal Brownian motion

$$\frac{\partial Q_\alpha}{\partial \tilde{S}} = \frac{1}{2} \frac{\partial^2 Q_\alpha}{\partial \tilde{\delta}^2} \quad (7)$$

by the substitution  $\tilde{S} = \Delta S^{2\alpha}$ .

### 2.2 The correlation

Imagine a halo is formed by the collapsing condition  $\delta(S_1) = \omega_1$  at  $S_1 = \sigma^2(M_1)$  with  $M_1$  being the halo mass. After some time the halo merges into a bigger halo with mass  $M_0 > M_1$  at  $S_0 = \sigma^2(M_0) < S_1$  by another collapsing condition  $\delta(S_0) = \omega_0 < \omega_1$ . The following question needs to be

<sup>1</sup> There are many anomalous random walks such as the fractal time process (Lutz 2001) which have the same scaling feature and are classified as sub-diffusion. The FBM is the simplest one of them.

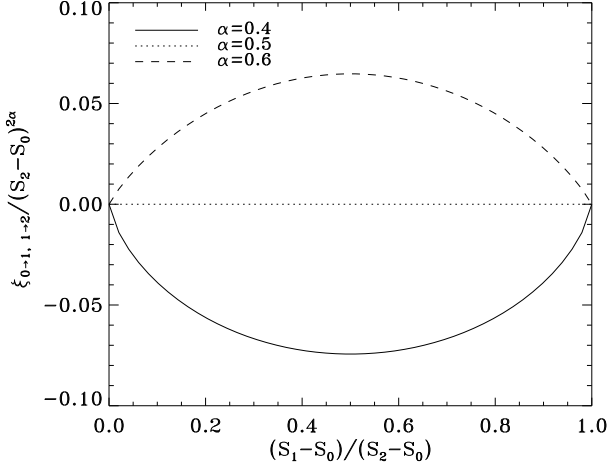


**Figure 1.** Correlation functions between successive halo merging steps (Eq.9).

addressed: how the formation event by  $\omega_0$  at  $S_0$  is correlated with the past merging process of  $\omega_1 - \omega_0$  within  $S_1 - S_0$ ?

If this process is approximated by the FBM, the correlation function can be easily calculated with Eq. (3). We have

$$\begin{aligned} \xi_{0,0 \rightarrow 1} &= \langle (\omega_0 - 0)(\omega_1 - \omega_0) \rangle \\ &= \frac{S_1^{2\alpha}}{2} \left[ 1 - \left( \frac{S_0}{S_1} \right)^{2\alpha} - \left( 1 - \frac{S_0}{S_1} \right)^{2\alpha} \right]. \end{aligned} \quad (8)$$

It is more instructive to capture the correlation between two successive merging steps:  $\omega_2 - \omega_1$  within  $S_2 - S_1$ , and  $\omega_1 - \omega_0$  within  $S_1 - S_0$  ( $S_2 > S_1 > S_0$ ,  $\omega_2 > \omega_1 > \omega_0$ ). The correlation function is similarly

$$\begin{aligned} \xi_{0 \rightarrow 1, 1 \rightarrow 2} &= \langle (\omega_2 - \omega_1)(\omega_1 - \omega_0) \rangle = \frac{(S_2 - S_0)^{2\alpha}}{2} \\ &\times \left[ 1 - \left( \frac{S_1 - S_0}{S_2 - S_0} \right)^{2\alpha} - \left( 1 - \frac{S_1 - S_0}{S_2 - S_0} \right)^{2\alpha} \right], \end{aligned} \quad (9)$$

which is positive when  $\alpha > 1/2$  and negative if  $\alpha < 1/2$ . Apparently,  $\alpha = 1/2$  causes null correlation (Fig. 1). Thus a unified paradigm is given by a single parameter controlled process: an anti-persistent FBM predicts that a merging step is anti-correlated with its immediate early occurrence of merging, and persistent FBM models positive correlation.

### 3 SPHERICAL COLLAPSE

#### 3.1 Conditional mass function

It is quite straightforward to solve the diffusion equation in spherical collapse model, we can actually copy the solution in the literatures (e.g. Bond et al. 1991; Lacey & Cole 1993). Spherical collapse is equivalent to employ the boundary condition that there is a fixed absorbing barrier of height  $\tilde{\delta}_c = \omega_1 - \omega_0 > 0$  to the reformed random walk described by Eq. (7). The number of trajectories of the reformed walk within  $(\tilde{\delta}, \tilde{\delta} + d\tilde{\delta})$  at  $\tilde{S}$  is

$$Q_\alpha d\tilde{\delta} = \frac{1}{\sqrt{2\pi\tilde{S}}} \left[ e^{-\tilde{\delta}^2/2\tilde{S}} - e^{-(\tilde{\delta}-2\tilde{\delta}_c)^2/2\tilde{S}} \right] d\tilde{\delta}, \quad (10)$$

and the number of trajectories absorbed by barrier within  $(\tilde{S}, \tilde{S} + d\tilde{S})$  is given by

$$\begin{aligned} f(\tilde{S}, \tilde{\delta}_c) d\tilde{S} &= -d\tilde{S} \frac{\partial}{\partial \tilde{S}} \int_{-\infty}^{\tilde{\delta}_c} Q_\alpha d\tilde{\delta} \\ &= \frac{\tilde{\delta}_c}{\sqrt{2\pi}} \tilde{S}^{-3/2} \exp\left(-\frac{\tilde{\delta}_c^2}{2\tilde{S}}\right) d\tilde{S}, \end{aligned} \quad (11)$$

which directly yields the universal conditional halo mass function

$$\begin{aligned} f(S_1 - S_0, \omega_1 - \omega_0) dS_1 &= f(S_1, \omega_1 | S_0, \omega_0) dS_1 \\ &= \frac{2\alpha}{\sqrt{2\pi}} \frac{\omega_1 - \omega_0}{(S_1 - S_0)^{\alpha+1}} \exp\left(-\frac{(\omega_1 - \omega_0)^2}{2(S_1 - S_0)^{2\alpha}}\right) dS_1. \end{aligned} \quad (12)$$

If  $\alpha = 1/2$  we recover the Eq. (2.15) in Lacey & Cole (1993).

The conditional mass function is in fact more fundamental than the mass function, since the mass function can be recovered from the conditional mass function by setting the limit  $S_0 \rightarrow 0, \omega_0 \rightarrow 0$  (Pan 2007),

$$f(S, \delta_c) dS = \frac{2\alpha}{\sqrt{2\pi}} \frac{\delta_c}{S^{\alpha+1}} \exp\left(-\frac{\delta_c^2}{2S^{2\alpha}}\right) dS. \quad (13)$$

Thus, prompted by the relation between mass function and conditional mass function, we recognize that there is a systematical effect due to the finite volume of simulations. This can lead to an underestimate of the halo mass function in the large mass regime (more details are discussed in Appendix A). Recall that the halo model tends to over-estimate the amplitude of the three point correlation function of dark matter, which can be corrected (at least partly) by applying certain arbitrary high mass cut-off to the halo mass function (Wang et al. 2004; Fosalba et al. 2005). To predict the three point correlation function of a simulation, a better approach would be to use the halo mass function of Eq. (A1) to include the finite volume effects.

#### 3.2 Merger rate

Now we will consider the merger rate function in line with Lacey & Cole (1993). For a trajectory which has experienced a first up-crossing over  $\omega_1$  at  $S_1$ , the conditional probability of having a first up-crossing over  $\omega_2$  ( $\omega_2 < \omega_1$ ) at  $S_2$  ( $S_2 < S_1$ ) in the interval  $dS_2$  is given by the Bayes formula,

$$\begin{aligned} f(S_2, \omega_2 | S_1, \omega_1) dS_2 &= \frac{f(S_1, \omega_1 | S_2, \omega_2) dS_1 f(S_2, \omega_2) dS_2}{f(S_1, \omega_1) dS_1} \\ &= \frac{2\alpha}{\sqrt{2\pi}} \frac{\omega_2(\omega_1 - \omega_2)}{\omega_1} \left[ \frac{S_1}{S_2(S_1 - S_2)} \right]^{\alpha+1} \\ &\times \exp\left[-\frac{1}{2} \left( \frac{(\omega_1 - \omega_2)^2}{(S_1 - S_2)^{2\alpha}} + \frac{\omega_2^2}{S_2^{2\alpha}} - \frac{\omega_1^2}{S_1^{2\alpha}} \right)\right], \\ &(\omega_1 > \omega_2, S_1 > S_2). \end{aligned} \quad (14)$$

This function is interpreted as the probability that a halo of mass  $M_1$  at time  $t$  will merge to build a halo of mass between  $M_2$  and  $M_2 + dM_2$  at time  $t_2 > t_1$ . The mean transition rate is obtained from it by setting  $t_2 \rightarrow t_1$  (equivalently  $\omega_2 \rightarrow \omega_1 = \omega$ ),

$$\begin{aligned} \frac{d^2 p(S_1 \rightarrow S_2 | \omega)}{dS_2 d\omega} dS_2 d\omega &= \frac{2\alpha}{\sqrt{2\pi}} \left[ \frac{S_1}{S_2(S_1 - S_2)} \right]^{\alpha+1} \\ &\times \exp\left[-\frac{\omega^2}{2} \frac{S_1^{2\alpha} - S_2^{2\alpha}}{S_1^{2\alpha} S_2^{2\alpha}}\right] dS_2 d\omega. \end{aligned} \quad (15)$$

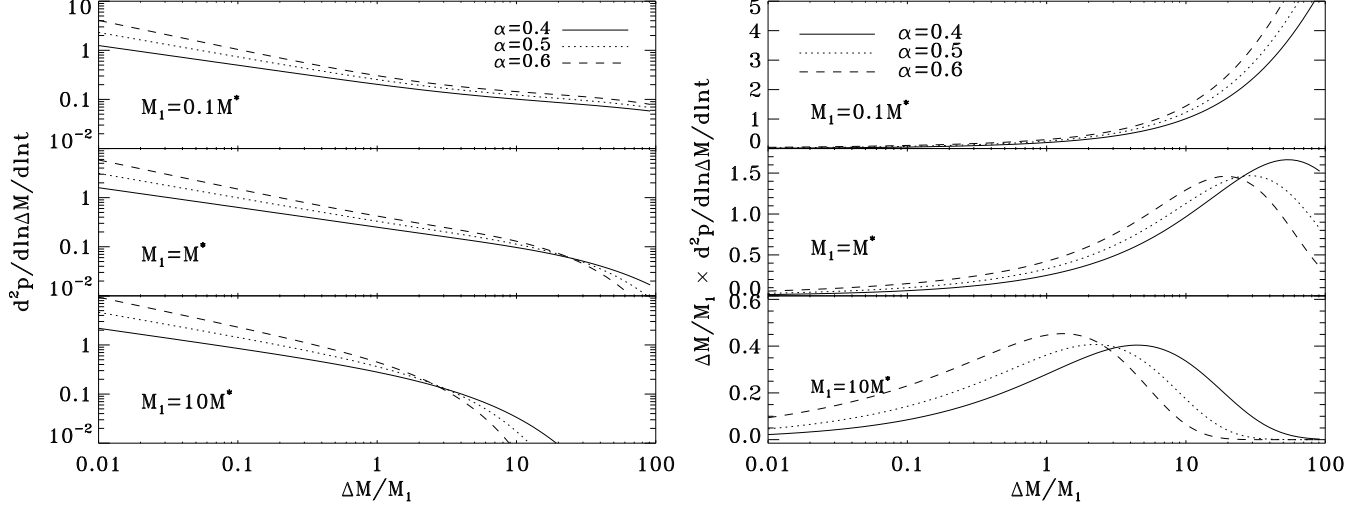


**Figure 2.** Halo merger rate (left panel) and accretion rate (right panel) computed with Eq. (16). The accretion rate is simply  $\Delta M/M_1 \times d^2p/d\ln\Delta M/d\ln t$ . Hereafter  $M^* = 10^{13} M_\odot$ .

Therefore the merger rate, i.e. the probability that a halo of mass  $M_1$  accretes a clump of mass  $\Delta M = M_2 - M_1$  within time  $d\ln t$  (corresponding to  $d\omega$ ), is

$$\begin{aligned}
 & d^2p(M_1 \rightarrow M_2|t)/d\ln\Delta M d\ln t \\
 &= 2\sigma(M_2)\Delta M \left| \frac{d\sigma_2}{dM_2} \right| \left| \frac{d\omega}{d\ln t} \right| \frac{d^2p(S_1 \rightarrow S_2|\omega)}{dS_2 d\omega} \\
 &= 2\alpha \sqrt{\frac{2}{\pi}} \frac{\Delta M}{M_2} \left| \frac{d\ln\delta_c}{d\ln t} \right| \left| \frac{d\ln\sigma_2}{d\ln M_2} \right| \frac{\delta_c(t)}{\sigma_2^{2\alpha}} \quad (16) \\
 &\times \left( \frac{\sigma_1^2}{\sigma_1^2 - \sigma_2^2} \right)^{\alpha+1} \exp \left[ -\frac{\delta_c^2}{2} \left( \frac{1}{\sigma_2^{2\alpha}} - \frac{1}{\sigma_1^{2\alpha}} \right) \right].
 \end{aligned}$$

In Figure 2 the halo merger rates of different masses as predicted by Eq. (16) are plotted for comparison. Three models are presented: an anti-persistent FBM of  $\alpha = 0.4$ , the standard normal Brownian motion of  $\alpha = 0.5$  and a persistent FBM of  $\alpha = 0.6$ .

For halo progenitors of the typical mass scale  $M_1 = M^*$ , the merger rate and halo accretion rate increases with increasing  $\alpha$  at small  $\Delta M/M_1$ , but at very large mass ratios ( $\Delta M/M_1 > 25$ ) the case is reversed.

This is also true for more massive progenitor masses ( $M_1 = 10M^*$ ), but here the transition point in the mass ratio is smaller:  $\Delta M/M_1 = 3$ .

For the less massive progenitors,  $M_1 = 0.1M^*$ , the transition point is very high, that in the whole plotted range (up to  $\Delta M/M_1 = 100$ ), the models with greater Hurst exponent always have greater merger and accretion rate.

### 3.3 Halo formation time distribution

The formation time (redshift) of a halo is the time (redshift) when its major progenitor contains half of the halo mass. According to the counter argument of LC93, the cumulative distribution of halo formation time, i. e. the probability that a halo of mass  $M_0$  at redshift  $z_0$  is formed at redshift larger

than  $z_f$ , can be acquired by

$$P(> z_f) = \int_{S_0}^{S_h} \frac{M_0}{M(S_1)} f(S_1, \delta_c(z_f)|S_0, \delta_c(z_0)) dS_1 \quad (17)$$

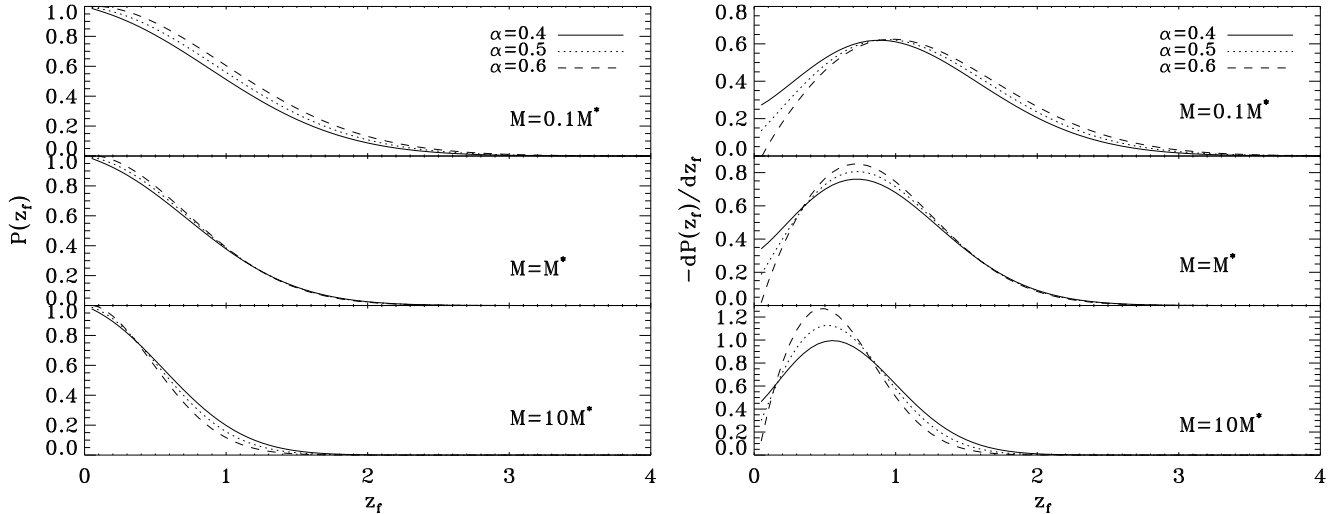
where  $S_0 = S(M_0)$  and  $S_h = S(M_0/2)$ . The halo formation time distribution is simply given by the differentiation  $-dP(z_f)/dz_f$ .

Figure 3 shows the predictions of the halo formation redshift distribution for difference masses. In general smaller halos have more extended formation time distribution than that of larger halos, in agreement with the results of Lin et al. (2003). For  $\alpha > 1/2$ , the halo formation redshift distribution is more concentrated than the  $\alpha = 1/2$  case, and for  $\alpha < 1/2$  the halo formation redshift distribution is more extended. This seems to be in accordance with our finding that the merger rate is greater for larger  $\alpha$ .

As can be seen, the detailed effects of incorporating correlation between merging steps are intricate, varying with the halo mass. Impact on the halo formation time distribution is small for those halos with masses around  $M^*$ , and it becomes apparent only when halo mass deviates significantly from  $M^*$ . The impact is also different for halos with small masses and large masses. Compared with the results given by the standard excursion set theory ( $\alpha = 1/2$ ),

(i)  $M \ll M^*$ : negative correlation ( $\alpha < 1/2$ ) shifts the halo formation time distribution curve to the side of smaller  $z_f$ , which means that the younger halos are more abundant and the older ones are less abundant; whilst for positive correlation ( $\alpha > 1/2$ ) the older ones are more abundant;

(ii)  $M > M^*$ : the impact of the correlation is opposite to the case of small halo mass, negative correlation ( $\alpha < 1/2$ ) boosts more halos to form at an earlier time while positive correlation ( $\alpha > 1/2$ ) induces more halos to form at a later time.



**Figure 3.** Halo formation time distributions for halos at  $z = 0$  with mass of 0.1, 1 and  $10M^*$ , which are predicted by the modified excursion set theory of different  $\alpha$  assuming spherical collapse. The left panel is the cumulative distribution.

## 4 ELLIPSOIDAL COLLAPSE

### 4.1 Moving barriers

The spherical collapse model is perhaps accurate at high redshift e.g. the re-ionization era. However, as shown by simulations, at low redshift the collapse of a clump of mass is ellipsoidal. For the excursion set theory, the general collapse condition for halo formation is not a constant  $\delta_c$  any more, but a moving barrier  $\mathcal{B}(S)$ .

Imposing a moving barrier on the random walk of  $(\tilde{\delta}, \Delta S)$  described by Eq. (6) is equivalent to the case of placing a constant barrier boundary condition to the diffusion equation with an extra drifting term (Zentner 2007). In our case of FBM, the Fokker-Planck equation turns out to be

$$\frac{\partial Q_\alpha}{\partial \Delta S} = \alpha \Delta S^{2\alpha-1} \frac{\partial^2 Q_\alpha}{\partial \tilde{\delta}^2} + \frac{\partial \Delta \mathcal{B}}{\partial \Delta S} \frac{\partial Q_\alpha}{\partial \tilde{\delta}} \quad (18)$$

where  $\Delta \mathcal{B} = \mathcal{B}(S_1) - \mathcal{B}(S_0)$ . Unfortunately this equation can be solved analytically only for a few very special cases (see Appendix B).

### 4.2 Conditional mass function: the Sheth-Tormen approximation

Although we do not have analytical solution of Eq. (18), it could be solved with the numerical method of Zhang & Hui (2006). However, this is inconvenient for general explorations. Here we borrow the pragmatic approach of Sheth & Tormen (2002), the conditional mass function is then approximated by

$$f(S_1 - S_0) dS_1 = dS_1 \frac{2\alpha}{\sqrt{2\pi}} \frac{|T(S_1, z_1 | S_0, z_0)|}{(S_1 - S_0)^{\alpha+1}} \times \exp \left\{ -\frac{[\mathcal{B}(S_1, z_1) - \mathcal{B}(S_0, z_0)]^2}{2(S_1 - S_0)^{2\alpha}} \right\}, \quad (19)$$

in which

$$T(S_1 | S_0) = \sum_{n=0}^5 \frac{(S_0 - S_1)^n}{n!} \frac{\partial^n [\mathcal{B}(S_1) - \mathcal{B}(S_0)]}{\partial S_1^n} \quad (20)$$

and

$$\mathcal{B}(S, z) = \sqrt{q} \delta_c(z) \left[ 1 + b \left( \frac{S}{q \delta_c^2(z)} \right)^\gamma \right] \quad (21)$$

with  $q = 0.707$ ,  $b = 0.485$  and  $\gamma = 0.615$  (Sheth et al. 2001; Sheth & Tormen 2002).

Inspired by the results given in Appendix B, it is probably more appropriate to use

$$T = \sum_n \frac{(-\tilde{S})^n}{n!} \frac{\partial^n \Delta \mathcal{B}}{\partial S^n} \quad (22)$$

with  $\tilde{S} = (S_1 - S_0)^{2\alpha}$  in Eq. 19. Testing the two approximation methods numerically, we found that the actual difference between the two is in fact very small. So we opted to use the numerically simpler Eq. (20).

In figure 4 we compare our prediction on the conditional mass function with that measured from the Millennium Simulation (Cole et al. 2008)<sup>2</sup> at  $z_0 = 0, z_1 = 0.5, 1, 2, 4$ , for halos of masses  $M_0 = 0.1, 3.16, 100M^*$ . It is indeed very interesting to notice that the performance of the original Sheth-Tormen approach (Eq. 19 of  $\alpha = 1/2$ ) is fairly good though not as remarkable as the fitting function of Cole et al. (2008). It is surprising that Cole et al. (2008) extrapolated the Sheth-Tormen mass function for the conditional mass function in ellipsoidal collapse model, in spite of the one actually proposed in Sheth & Tormen (2002).

From Figure 4 we can see that the effects of correlation between merging steps gradually decrease with time, with halo formation becoming sensitive to the correlation at high redshift. Except in cases of high redshifts and of extremely high halo mass, it appears that positive correlation ( $\alpha > 1/2$ ) is preferred by the simulation in  $\Lambda$ CDM universe. Nevertheless, one must be cautious to this result, as the measurement presented is rather crude and lacks error bars. Its accuracy is not sufficient to justify with confidence whether

<sup>2</sup> The data is publicly available at [http://star-www.dur.ac.uk/~cole/merger\\_trees](http://star-www.dur.ac.uk/~cole/merger_trees)

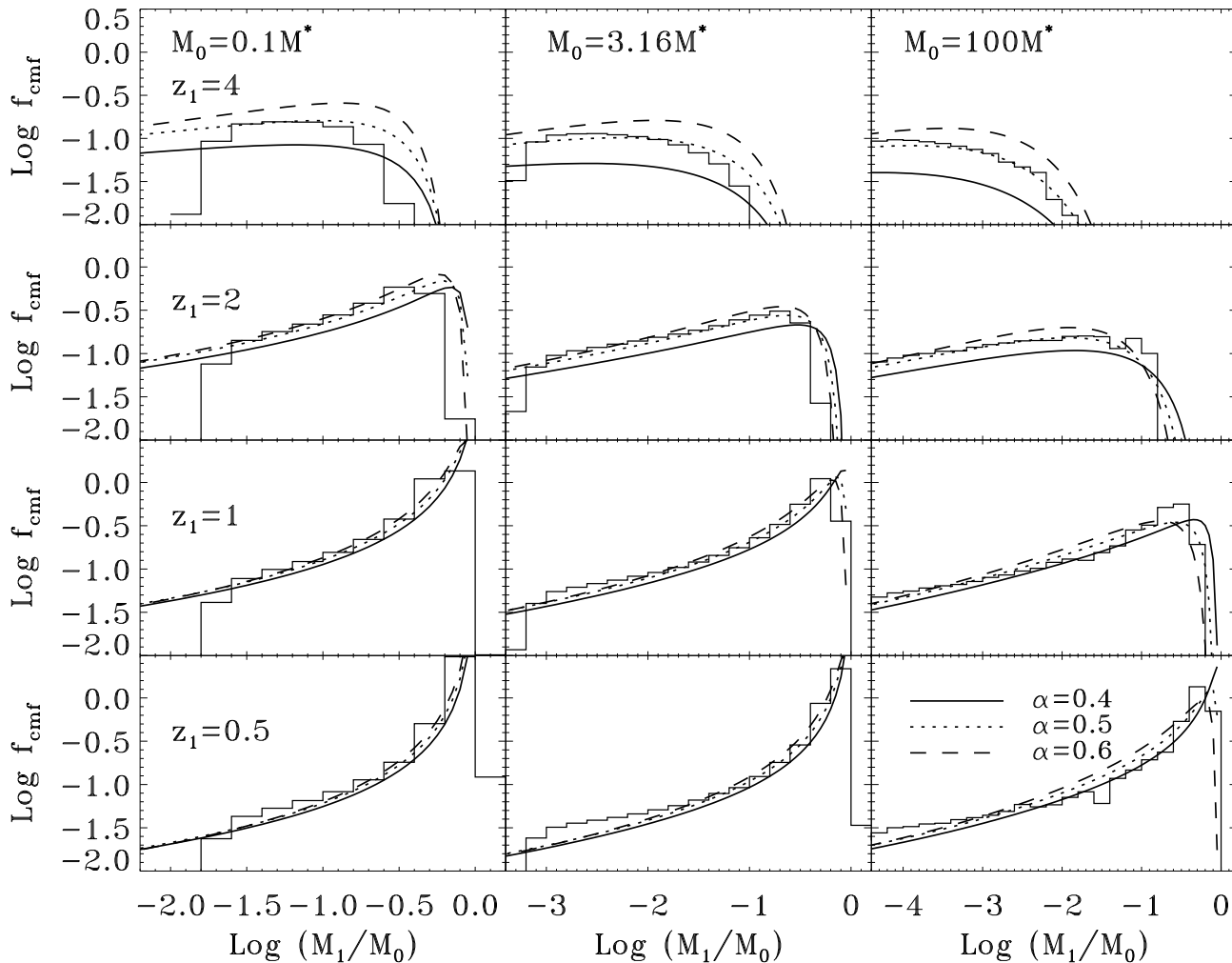


**Figure 4.** Conditional mass functions of progenitor halos at redshift  $z_1 = 0.5, 1, 2, 4$  (identical for each row) for three different halo masses  $M_0$  (each column has the same mass). Histograms are the results from the Millennium Simulation given by Cole et al. (2008), while lines are predictions by Eq. (19) of three different values of  $\alpha$  as indicated.

the correlation between merging steps is positive, negative or zero.

### 4.3 Halo formation time distribution

The halo formation time distribution is recalculated with the modified excursion set theory in ellipsoidal collapse model and the results displayed in Figure 5. Although the halo formation time distributions are modulated significantly by the non-constant barrier, its dependence on  $\alpha$  does not change, and demonstrates similar trends as the spherical models predicts: positive correlation results in more old small mass halos and more young large mass halos, while the effects of the negative correlation are to the contrary.

Giocoli et al. (2007) calculated the cumulative distribution of halo formations time and compared with GIF2 simulation. They found that the median formation redshift of halos of mass less than  $M^*$  extracted from the simulation is larger than that predicted by the Sheth-Tormen formula, even after some numerical improvement. Combined

with our discovery of effects of correlation, it seems that the discrepancy can be explained by the existence of a positive correlation between adjacent merging steps.

## 5 CONCLUSIONS AND DISCUSSION

In this work the FBM is formally incorporated in the excursion set theory, to account for possible correlations between merging steps of halo formation. Such modification is minimal but provides a unified theoretical frame to investigate the effects of correlation. More specifically, the correlation depends on the Hurst exponent  $\alpha$ , for  $\alpha < 1/2$ , the correlation between adjacent merging steps is negative, for  $\alpha > 1/2$  the correlation is positive, while  $\alpha = 1/2$  is reduced to the standard case of null correlation.

We calculated the conditional mass functions in models of the spherical collapse and the ellipsoidal collapse. Different collapsing conditions do not change the relative effects of correlations. It is revealed that for a typical progenitor of

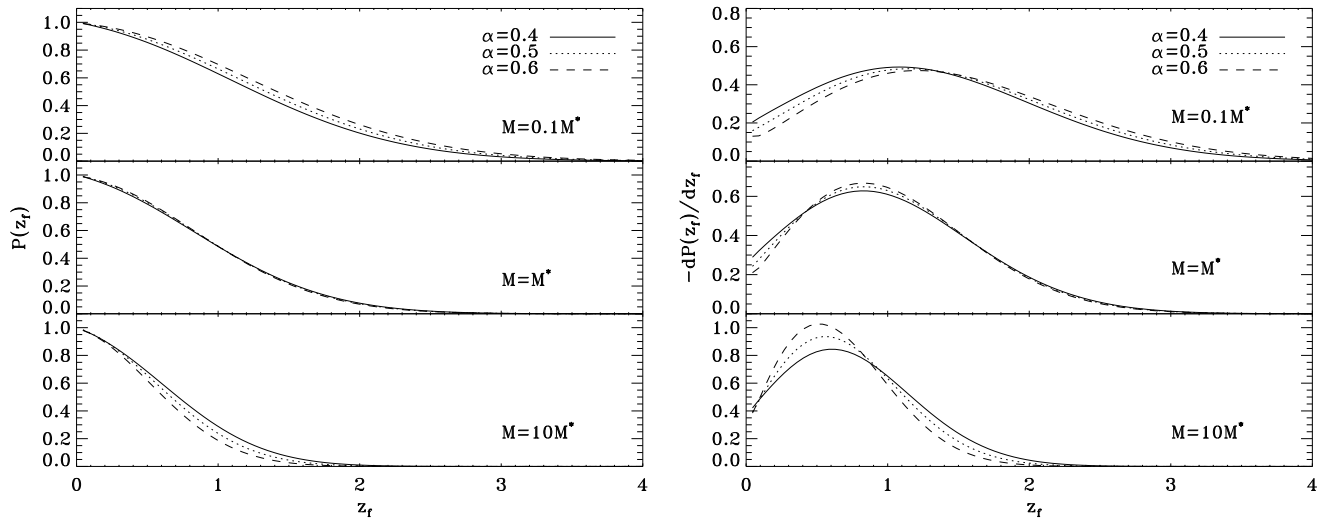


**Figure 5.** Halo formation time distributions for halos of masses 0.1, 1 and  $10M^*$  at  $z = 0$ , which are predicted by the modified excursion set theory of different  $\alpha$  in ellipsoidal collapse model. The left panel is the cumulative distribution.

$M^*$ , a positive correlation will boost the merger rate when the mass to accrete is less than  $\sim 25M^*$ , and negative correlation will significantly reduce such a rate. Accordingly we find that compared with the standard excursion set theory without correlation, positive correlation increases the aged population for small mass halos but produces more young members for large mass halos; while the negative correlation projects opposite effects to the halo formation. The same trend is also seen for other progenitor masses, although the transition mass ratio is greater for small progenitor masses and smaller for greater progenitor masses.

The results of the modified excursion set theory in ellipsoidal collapse model are checked with those measurements from simulations of Giocoli et al. (2007) and Cole et al. (2008). The comparison indicates that there is a sign of weak positive correlation, although not yet of significant confidence, as it is limited by the accuracy and dynamic ranges of their analysis. The conclusion appears to be in conflict with the claim of Pan (2007), but note that in that work the mass function was calculated with the spherical collapse model, which is not valid at most redshifts of concern. Besides, the main purpose of Pan (2007) is to show that the effect of correlation is not trivial.

The accuracy of the Sheth-Tormen approximation to the ellipsoidal collapse in the modified (FBM) excursion set theory has not been checked against rigorous numerical solutions. However, since the actual correlation is weak, i.e.  $\alpha$  only deviates from 1/2 slightly, the approximation suffices for general qualitative discussion. Calibration and subsequent improvement of the approximation with numerical computation is of course needed for more precise analytical modeling and implementation in semi-analytical models of galaxy formation.

In this paper we explored the effects of correlations between mergers on the global halo formation process. It is of interests to actually check if such a correlation will lead to the assembly bias discovered by Gao et al. (2005), and whether it can explain the dependence of halo formation on the large scale environment.

A by product of our work is the discovery of a systematic effect in the mass function due to the finite volume of simulation. It explains why applying a high mass cut-off to the mass function can improve the halo model prediction on three point correlation function. A better approach in the halo model calculation of three point function is to shift the theoretical mass function according to the formulae given in Appendix A, this may lead to better agreement between simulation and analytical results.

## ACKNOWLEDGMENT

The authors acknowledge stimulating discussions with Pengjie Zhang, Jun Zhang, Weipeng Lin and Longlong Feng. JP is supported by the China Ministry of Science & Technology through 973 grant of No. 2007CB815402 and the NSFC through grants of Nos. 10643002, 10633040. YGW and XLC are supported by NSFC via grants 1052314, 10533010, the CAS under grant KJCX3-SYW-N2, and the Ministry of Science & Technology via 973 grant of 2007CB815401. LT acknowledges the financial support of the Leverhulme Trust (UK).

## REFERENCES

- Bond J. R., Cole S., Efstathiou G., Kaiser N., 1991, ApJ, 379, 440
- Cole S., Helly J., Frenk C. S., Parkinson H., 2008, MNRAS, 383, 546
- Cuesta A. J., Prada F., Klypin A., Moles M., 2007, astro-ph/0710.5520
- Feder J., 1988, Fractals. Plenum Press, New York
- Fosalba P., Pan J., Szapudi I., 2005, ApJ, 632, 29
- Gao L., Springel V., White S. D. M., 2005, MNRAS, 363, L66
- Giocoli C., Moreno J., Sheth R. K., Tormen G., 2007, MNRAS, 376, 977
- Lacey C., Cole S., 1993, MNRAS, 262, 627

- Lin W. P., Jing Y. P., Lin L., 2003, MNRAS, 344, 1327  
 Lukić Z., Heitmann K., Habib S., Bashinsky S., Ricker P. M., 2007, ApJ, 671, 1160  
 Lutz E., 2001, Phys. Rev. E, 64, 051106  
 Pan J., 2007, MNRAS, 374, L6  
 Reed D. S., Bower R., Frenk C. S., Jenkins A., Theuns T., 2007, MNRAS, 374, 2  
 Sheth R. K., 1998, MNRAS, 300, 1057  
 Sheth R. K., Mo H. J., Tormen G., 2001, MNRAS, 323, 1  
 Sheth R. K., Tormen G., 2002, MNRAS, 329, 61  
 Wang Y., Yang X., Mo H. J., van den Bosch F. C., Chu Y., 2004, MNRAS, 353, 287  
 Warren M. S., Abazajian K., Holz D. E., Teodoro L., 2006, ApJ, 646, 881  
 Zentner A. R., 2007, International Journal of Modern Physics D, 16, 763  
 Zhang J., Hui L., 2006, ApJ, 641, 641

## APPENDIX A: FINITE VOLUME EFFECTS IN SMALL-BOX SIMULATIONS

N-body simulations are always performed in cubic boxes of finite size  $L_{sim}$ . By definition, the density contrast of whole the simulation box is zero, but the variance is not. Henceforth the measured mass function of simulation is conditional, determined by  $f(S_1 = S, \omega_1 = \delta_c | S_0(L_{sim}) \neq 0, \omega_0 = 0)$ . From Eq. (12) the explicit halo mass function of a simulation is then

$$f(\sigma, L_{sim}) d \ln \sigma = \frac{4\alpha}{\sqrt{2\pi}} \frac{\delta_c}{(\sigma^2 - \sigma_0^2)^\alpha} \frac{\sigma^2}{\sigma^2 - \sigma_0^2} \times \exp \left[ -\frac{\delta_c^2}{2(\sigma^2 - \sigma_0^2)^{2\alpha}} \right] d \ln \sigma, \quad (\text{A1})$$

where

$$S = \sigma^2 = (2\pi)^{-3} \int_{2\pi/L_{sim}}^{\infty} P(k) \widetilde{W} 4\pi k^2 dk,$$

and

$$S_0 = \sigma_0^2(L_{sim}) = (2\pi)^{-3} \int_{2\pi/L_{sim}}^{\infty} P(k) \widetilde{W}(k, L_{sim}) 4\pi k^2 dk.$$

The infrared cutoff in the integration for  $\sigma^2$  accounts for the deficiency of large scale power in finite box, which has already been identified as a systematic effect (e.g. Reed et al. 2007).

The difference between Eq. (A1) and Eq. (13) is shown in Fig. A1 for different box sizes. The fiducial model has  $\alpha = 0.436$ , by which the spherical model provides good approximation to the mass function of simulations in high mass region (Pan 2007). We can see that the finite volume effect becomes apparent only when  $-\ln \sigma > 0.2$ , i.e. in high mass regime, and the resulting fractional error quickly drops down to  $< 10\%$  for simulations of  $L_{sim} > 100h^{-1}\text{Mpc}$ .

Nowadays it is a very common practice to use simulations with boxes as small as  $< 50h^{-1}\text{Mpc}$  to extend the dynamic range. The finite volume effect demonstrated in Fig. A1 has to be taken into account for precision measurement. The necessary correction is actually very simple: the true measured mass function  $f(S)dS$  can be recovered by shifting the raw mass function  $f(S|S_0)dS$  along  $S$  by  $S_0$ . Note that there is a cosmic variance for  $S_0$ , for each

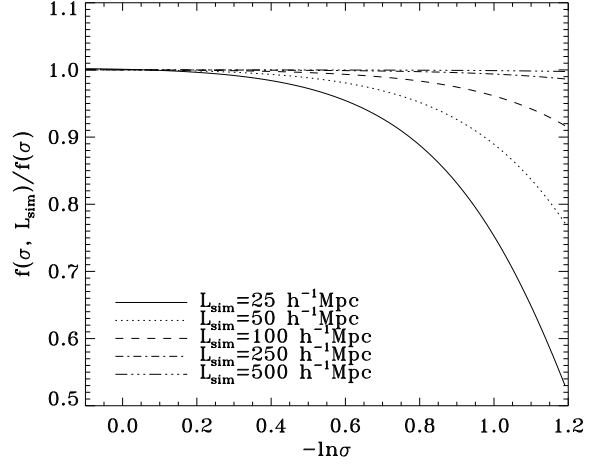


**Figure A1.** Deviation of mass functions in finite-sized simulations (Eq. A1) to Eq. (13). For the fiducial model  $\alpha = 0.436$ .  $L_{sim}$  is the size of the cubic box for simulation.  $\sigma_0$  is calculated with infrared cutoff in integration (see text), and a spherical top-hat window function in real space of radius  $L_{sim}/(4\pi/3)^{1/3}$ . Deviation is negligible in regime  $-\ln \sigma < 0.2$ .

individual realization of simulation one may need to calculate the individual  $S_0$  from the realization (Reed et al. 2007; Lukić et al. 2007).

## APPENDIX B: PSEUDO-LINEAR BARRIER:

$$\mathcal{B} = \delta_c + \beta S^{2\alpha}$$

Starting with Eq. (18), let  $S_0 = 0$  and  $S_1 = S > 0$ , a variable substitution  $\tilde{S} = S^{2\alpha}$  yields

$$\frac{\partial Q_\alpha}{\partial \tilde{S}} = \frac{1}{2} \frac{\partial^2 Q_\alpha}{\partial \tilde{\delta}^2} + \frac{1}{2\alpha S^{2\alpha-1}} \frac{\partial \mathcal{B}}{\partial S} \frac{\partial Q_\alpha}{\partial \tilde{\delta}} \quad (\text{B1})$$

If the barrier is  $\mathcal{B} = \delta_c + \beta S^{2\alpha}$ , the above nonlinear Fokker-Planck equation is further simplified to

$$\frac{\partial Q_\alpha}{\partial \tilde{S}} = \frac{1}{2} \frac{\partial^2 Q_\alpha}{\partial \tilde{\delta}^2} + \beta \frac{\partial Q_\alpha}{\partial \tilde{\delta}}, \quad (\text{B2})$$

which is the well known problem of a linear barrier upon the normal Brownian motion (Sheth 1998; Zentner 2007).

The probability of a trajectory that has the first barrier passage within  $(\tilde{S}, \tilde{S} + d\tilde{S})$  in the solution is given by

$$f(\tilde{S}) d\tilde{S} = \frac{\delta_c}{\sqrt{2\pi} \tilde{S}^{3/2}} \exp \left[ -\frac{(\beta \tilde{S} + \delta_c)^2}{2\tilde{S}} \right] d\tilde{S}, \quad (\text{B3})$$

from which the universal mass function is easily obtained

$$f(\sigma) d \ln \sigma = \frac{4\alpha}{\sqrt{2\pi}} \frac{\delta_c}{\sigma^{2\alpha}} \exp \left[ -\frac{(\delta_c + \beta \sigma^{4\alpha})^2}{2\sigma^{4\alpha}} \right] d \ln \sigma. \quad (\text{B4})$$

However, there is no analogous analytical expression for the conditional mass function under this type of barrier, as the barrier does not have the symmetry that a true linear barrier possesses: for any pair of points at  $S_0$  and  $S_1 > S_0$

$$\mathcal{B}_1 - \mathcal{B}_0 = \beta(S_1^{2\alpha} - S_0^{2\alpha}) \neq \beta(S_1 - S_0)^{2\alpha}. \quad (\text{B5})$$

This is why we call it *pseudo-linear*.